

(HUANJING KEXUE)

ENVIRONMENTAL SCIENCE

第39卷 第3期

Vol.39 No.3

2018

____ 中国科学院生态环境研究中心 主办

斜学出版社出版



环龙科豆 (HUANJING KEXUE)

ENVIRONMENTAL SCIENCE

第39 卷 第3期 2018年3月15日

次

DO/NH4 - N实现短程硝化过程中生物膜特性

赵青1, 卞伟1, 李军1*, 王文啸1, 孙艺齐1, 梁东博1, 张舒燕2

(1. 北京工业大学建筑工程学院, 北京 100124; 2. 神华集团中国节能减排有限公司, 北京 100011)

摘要:实验探究了短程硝化实现过程中生物膜特性的变化情况. 采用比值控制(DO/NH₄⁺-N)实现短程硝化,分别取亚硝酸盐积累率为10.27%、52.12%和93.54%时生物膜样品,利用荧光原位杂交(FISH)和激光共聚焦显微镜(CLSM)联用技术观察总菌、氨氧化菌(AOB)和亚硝酸盐氧化菌(NOB)数量和空间结构的变化,通过三维激发发射矩阵(EEM)观察胞外聚合物分泌和成分变化情况. 比值控制成功富集 AOB,并可在 NOB 未洗脱完全的情况下实现短程硝化. 异养菌和硝化菌共存于生物膜内上,异养细菌在外层,硝化菌分布在生物膜表面 6~25 μm. 短程硝化实现的过程中,AOB/NOB 值逐步增长,稳定运行时期比值高达 15.56. 反应器运行过程中,EPS 和微生物菌群变化息息相关. 微生物活性下降,EPS 分泌减少;短程硝化稳定运行时期,NOB 等不耐高亚硝酸的菌群衰亡,芳香性蛋白质荧光强度降低. 但三维荧光光谱显示,短程硝化实现过程中 EPS 化学成分变化不明显.

关键词:短程硝化;生物膜;硝化细菌;胞外聚合物

中图分类号: X703.5 文献标识码: A 文章编号: 0250-3301(2018)03-1278-08 DOI: 10.13227/j. hjkx. 201708055

Characteristics of Biofilm During the Transition Process of Complete Nitrification and Partial Nitrification

ZHAO Qing¹, BIAN Wei¹, LI Jun¹*, WANG Wen-xiao¹, SUN Yi-qi¹, LIANG Dong-bo¹, ZHANG Shu-yan² (1. College of Architecture and Civil Engineering, Beijing University of Technology, Beijing 100124, China; 2. China Energy Saving and Emission Reduction Limited Company of Shenhua Group, Beijing 100011, China)

Abstract: The objective of the study was to investigate the change of biofilm characteristics when implementing the procedure of partial nitrification. A ratio control strategy (DO/NH₄⁺-N) was taken to achieve partial nitrification, and biofilm samples were obtained at 10.27%, 52.12%, and 93.54% of the nitrite accumulation rate. The amount and spatial distribution of total bacteria, ammonia oxidizing bacteria (AOB), and nitrite oxidative bacteria (NOB) were observed by fluorescence in situ hybridization (FISH) and confocal laser scanning microscope (CLSM) through a three-dimensional excitation emission matrix (EEM) to observe the secretion and composition changes of extracellular polymer substances. Ratio control successfully enriched AOB and achieved partial nitrification under conditions when NOB was not completely washed. Heterotrophic bacteria and nitrifying bacteria coexist in the biofilm. The heterotrophic bacteria were in the outer layer, but nitrifying bacteria were distributed in the biofilm surface at 6-25 μm. During the process of short-range nitrification, the AOB/NOB value gradually increased, and the stable operation period was as high as 15.56. During the operation of the reactor, EPS and microbial flora changes are closely related. When microbial activity decreased, EPS secretion decreased. During the stable operation period of partial nitrification, NOB and other bacteria that are non-resistant to high nitrite nitrous acid declined, and the fluorescence intensity of aromatic protein-like bacteria decreased. However, the three-dimensional fluorescence spectra showed that the chemical composition of EPS was not obvious during the process of partial nitrification.

Key words: partial nitrification; biofilm; nitrifying bacteria; extracellular polymeric substances

传统硝化工艺首先在氨氧化菌(AOB)作用下,将铵态氮转化为亚硝态氮,然后通过亚硝酸盐氧化菌(NOB)使亚硝态氮氧化为硝态氮. 短程硝化将氨氮氧化控制在亚硝酸盐氮阶段,不仅可以节省25%曝气能耗,反硝化过程还可以减少有机碳源投加量^[1]. 近几年,学者对短程硝化的关注力度有所增加. 短程硝化的实现机理是利用 AOB 和 NOB 生理特性差异,使 AOB 的生长速率高于 NOB. 实现和维持短程硝化的技术手段主要有:高温、高 pH、高游离氨(FA)、高游离亚硝酸(FNA)、适宜的水力停留时间(HRT)、低溶解氧(DO). 本研究采用比值

控制^[2] 实现移动床生物膜反应器 (moving bed biofilm reactor, MBBR)工艺短程硝化. 短程硝化成功实现的关键因素是富集 AOB, DO 和NH₄⁺-N是 AOB 生长繁殖的主要基质, 故优先选取 DO 和出水 NH₄⁺-N质量浓度作为控制因素. Bartrolí 等^[3] 和 Jemaat 等^[4]认为比值控制策略可同时调控 DO 和出

收稿日期: 2017-08-07; 修订日期: 2017-09-01

基金项目: 国家水体污染控制与治理科技重大专项(2015ZX07202-

013)

作者简介: 赵青(1991~), 女, 硕士研究生, 主要研究方向为生物 膜短程硝化启动、破坏及稳定运行, E-mail:374343833@

* 通信作者,E-mail:jglijun@bjut.edu.cn

水NH₄ -N浓度,发挥氨抑制和氧抑制双重作用,最大程度可使氨氮 100% 氧化为亚硝态氮.目前,短程硝化的关注热点多在于实现方法和维持手段,对短程硝化微生物种群研究较少,且鲜有对短程硝化的实现过程中菌群差异进行对比分析.了解生物膜内短程硝化实现过程中菌群的空间分布规律和群落结构及功能的变化,对反应器尽快达到预期处理效果有一定的理论指导意义.

不同的短程硝化实现手段可影响胞外聚合物(EPS)的分泌和组成成分. 胞外聚合物(EPS)是细胞新陈代谢分泌的一种高分子聚合物,包裹在微生物细胞膜外面,是生物膜的重要组成部分,具有保护和维持生物膜的作用. EPS 的成分主要以蛋白质(PN)和多糖(PS)为主(约70%~80%),其余20%~30%为核酸、脂类和其他物质. EPS 成分和空间结构的改变,直接影响生物膜的亲和性、凝聚性和传质阻力等理化性能. 李延等[5]探究了 SBBR 反应器运行周期中 EPS 产生和变化特征,揭示了 EPS 在反应器运行中的重要作用. 因此,考虑到 EPS 在污水处理中的重要性,深入研究和辨识 EPS 主要成分,对更好地理解短程硝化的实现机理具有十分重要的意义. 但是,目前对这方面的研究较少.

荧光原位杂交(FISH)利用已知的携带荧光标记的特异寡核苷酸片段作为探针,与待测微生物DNA 依据碱基互补配对原则进行杂交,可对被测微生物种群进行定性、定位和半定量分析^[6].但由于传统荧光显微镜精确度不高,对荧光物质分析存在较大偏差,故 FISH 常与激光共聚焦显微镜技术(CLSM)联用. CLSM激光穿透性强,可对样本进行一定深度光学断层,更全面、形象地分析生物膜结构^[7].本研究利用 FISH 和 CLSM 联用技术,探究MBBR 反应器短程硝化实现过程中菌群演替和空间变化规律.三维激发发射矩阵(EEM)具有高选择性和不损坏样品等优点,广泛用于 EPS 测定.本文研究了在短程硝化实现过程中 EPS 的含量和组成的变化,并解析了不同时期生物膜样品荧光吸收类有机组成与浓度的变化特征.

1 材料与方法

1.1 反应器运行概况

本实验装置采用连续流反应器,如图 1 所示. 反应器为立方体结构,长×宽×高为 18 cm×12 cm×18 cm,有效体积约为 4.3L.反应器材质采用有机玻璃,底部设有曝气盘.用 DO 和 pH 探头在线监 测 DO、pH 值的变化. 生物膜载体采用鲍尔环,由高密度聚乙烯,辅以多种微量元素及改性剂加工而成,内部设有交叉支撑面,外部为波浪状沟棱,其主要技术参数为:密度 > 0.96 g·cm⁻³,规格 Φ25 mm×10 mm,有效表面积 > 400 m²·cm⁻³. 鲍尔环填充体积约为1 L. 成功挂膜后的鲍尔环上形成一层淡黄色薄膜.

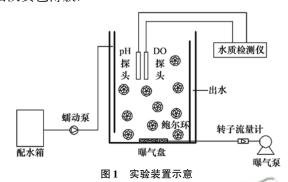


Fig. 1 Schematic diagram of experimental device

反应器直接填充已成功挂膜、并已连续运行 200 d 的鲍尔环,此时亚硝酸盐积累率(NAR)约为 5%. 此时,FISH 分析显示,AOB 约为 NOB 的 1% $\pm 1\%$. 进水水质采用人工配水,NH $_4^+$ -N(NH $_4$ CI)质量浓度约为 60 mg·L $^{-1}$,COD(CH $_3$ COONa)值 90 mg·L $^{-1}$,磷(KH $_2$ PO $_4$)为 2 mg·L $^{-1}$,通过调节投加 NaHCO $_3$ 量,维持 pH 为 7.8 ~ 8.2. 同时添加适量营养液,为微生物生理活动提供所需微量元素. MBBR 工艺采用比值控制方式实现短程硝化,通过调节转子流量计和蠕动泵,控制曝气量和 HRT,从而调节 DO 和出水 NH $_4^+$ -N浓度,改变和维持 DO/NH $_4^+$ -N值.

1.2 水质检测

 NH_4^+ -N:纳氏试剂分光光度法; NO_2^- -N:N-(1-萘基)-乙二胺分光光度法; NO_3^- -N:麝香草酚分光光度法; DO_{pH} 和 T 采用在线探头检测(WTW,德国). 定义亚氮积累率为 $NAR = NO_3^-$ -N/(NO_2^- -N+ NO_3^- -N),其中 NO_3^- -N、 NO_2^- -N均指由 NH_4^+ -N氧化而来的部分. MLSS、MLVSS:超声波(45 kHz,120 W,2~3 min)剥落生物膜,离心(10 000 g,15 min)后重量法测量.

1.3 生物膜分析

1.3.1 荧光原位杂交(FISH)

本实验采用荧光原位杂交技术(FISH)和共聚 焦激光显微镜技术(CLSM)分析生物膜内总菌、 AOB 和 NOB 的空间分布规律. 样品用1×PBS 溶液 清洗3次, 然后置于4%多聚甲醛溶液于4℃固定1 ~3 h,固定后样品可在 -20℃环境下保存 6 个月.加入杂交缓冲液和探针的混合液,放入 46℃杂交箱杂交 2~3 h,再用清洗缓冲液清洗 20 min^[8,9].杂交后样品加入抗荧光衰减剂,避光保存,依次在共

聚焦激光扫描显微镜(FV1200, Olympus, Japan)下观察. 实验中探针主要特性^[10,11]如表 1 所示,探针上所携带荧光染料均在 5'末端标记,根据荧光颜色的不同来区分细胞种类.

表 1 实验所用 FISH 探针的主要特性

Table 1 Main characteristics of the FISH probe used in the experiment

探针	特异性	发射波长/nm	激发波长/nm	荧光染料	颜色
EUB338	Most bacteria	525. 0	488. 1	FAM	绿
EUB338 II	Bacterial lineages not covered by probe EUB338 and EUB338 Ⅲ	525. 0	488. 1	FAM	绿
EUB338 Ⅲ	Bacterial lineages not covered by probe EUB338 and EUB338 $ \mathrm{I\hspace{1em}I}$	525. 0	488. 1	FAM	绿
NSO190	β -subgroup ammonia oxidizing bacteria	595. 0	560. 8	Cy3	红
NIT3	Nitrobacter	700. 0	646. 8	Cy5	紫

1.3.2 CLSM 荧光染色观察

用可以穿透细胞膜、对细胞毒性较低的荧光染料 Hoechst 33342,标记活细菌;碘化丙啶(propidium iodide, PI)可穿过破损细胞膜,对细胞核染色,但不能通过活细胞膜^[12],标记死细胞.异硫氰酸荧光素(fluorescein isothiocyanate, FITC)是氨基标记荧光染料,具有较强的蛋白结合能力,本实验中用来指示胞外蛋白质. Hoechst 33342和 PI 染色同一样品,FITC 单独染色. 生物膜样品荧光染

色所用染料、激发波长、发射波长和使用浓度见表 2. 具体染色过程如下:取生物膜样品用 $1 \times PBS$ 清洗 3 遍; 首先加入 Hoechst 33342 (10 μ L, 0.01 $mg \cdot mL^{-1}$)染色 30 min(置于 200 $r \cdot min^{-1}$ 恒温摇床中,以下染色过程条件相同);随后加入 $PI(1 \mu L, 0.02 mg \cdot mL^{-1})$ 染色 30 min; 再加入 $FITC(10 \mu L, 10 mg \cdot mL^{-1})$ 染色 1 h; 上述每种染料染色结束后均用 $1 \times PBS$ 清洗 3 遍. 最后用 FV1200 显微镜观察样品.

表 2 CLSM 所用荧光染料的主要特性

Table 2 Main characteristics of fluorescent dyes used in the CLSM

/ 0 / 1/1 //		9 11 1 19 19			
染料	特异性	发射波长/nm	激发波长/nm	颜色	浓度/mg·mL ⁻¹
Hoechst 33342	活细胞	450.0	402. 8	蓝色	0. 01
PI (死细胞	595.0	560. 8	红色	0. 02
FITC	胞外蛋白质	525. 0	488. 1	绿色	10

1.3.3 高通量测序^[13]

分别取短程硝化不同时期鲍尔环样品,将生物膜从载体上剥离,离心预处理后,送往上海生工进行高通量测序分析.

1.3.4 EPS 测定

预处理方法同 1.3.3 节,离心得到的沉淀物置于 PBS 中,将混浊悬浮液水浴 80% 加热 0.5 h,再次离心所得上清液即为 EPS 样品. 所得样品一部分用于 PN、PS 检测: PN 采用考马斯亮蓝法,PS 采用蒽酮法;一部分用于三维荧光光谱测定:采用荧光光谱仪(F-7000,日本日立),设置激发(E_x)波长 $200\sim400$ nm,每次增加 5 nm,发射(E_m)波长 $240\sim600$ nm,波长间隔 2 nm,激发光和发射光的狭缝均为 5 nm,扫描速度为 1 200 nm·min $^{-1}$.

2 结果与讨论

2.1 MBBR 反应器运行工况

接种鲍尔环在高曝气(DO 为 7~8 mg·L⁻¹)下

实现全程硝化. 图 2 显示 MBBR 反应器运行期间 NO_3^--N 、 NO_2^--N 、 $NH_4^+-N和$ NAR 的变化. 反应器运行期间调节 DO 约为 2. 0 $mg \cdot L^{-1}$ 和出水 NH_4^+-N 浓度 约 8. 0 $mg \cdot L^{-1}$,DO/ $NH_4^+-N=0$. 25 ± 0. 05. 经过 20 d 运行,成功实现短程硝化,NAR 在第 20 d 达

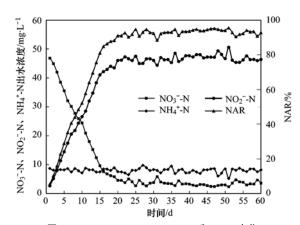


图 2 NO_3^- -N、 NO_2^- -N、 NH_4^+ -N和 NAR 变化

Fig. 2 Variation of NO_3^- -N, NO_2^- -N, NH_4^+ -N and NAR

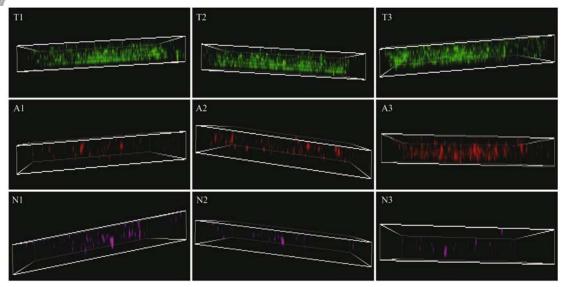
90. 54%,说明采用比值控制(DO/NH₄⁺-N)可高效迅速实现 MBBR 工艺短程硝化. 根据亚硝酸盐积累情况,1~20 d 为短程硝化实现阶段,21~60 d 为短程硝化稳定运行阶段. 前 20 d,出水NO₃⁻-N浓度由 46. 83 mg·L⁻¹降为 4. 58 mg·L⁻¹,NO₂⁻-N浓度由 2. 69 mg·L⁻¹逐渐升高至 46. 03 mg·L⁻¹. 短程硝化稳定运行阶段,出水 NO₃⁻-N 、NO₂⁻-N 浓度约为(3. 62 ± 0. 1) mg·L⁻¹和(46. 64 ± 0. 2) mg·L⁻¹,NAR值均在 90%以上,说明生物膜上 AOB活性很高,NOB处于抑制状态. 分别取 NAR = 10. 27%(2 d)、NAR = 52. 12%(10 d)和 NAR = 93. 54%(45 d)时样品生物膜进行检测分析.

2.2 生物膜中微生物菌落三维空间分布

EUB338、EUB338 Ⅲ 、EUB338 Ⅲ 三者标记的细菌总和记为总菌,携带 FAM 荧光染料,激发后呈现绿色;NSO190 为β-氨氧化菌的通用探针,采用Cy3 荧光染料标记,激发后呈红色;NIT3 探针 5′端用Cy5 染料标记,激发和发射波长分别为 630 nm和 670 nm,呈紫色。随机选取样品上荧光强度较强的某点,进行分层扫描,利用 FV10-ASW 4.20 Viewer 软件对图像三维重组。图 3 为样品荧光原位杂交 3D 照片,其中 T1、T2、T3 是 NAR 为10.27%、52.12%和 94.53% 这 3 个时期生物膜总菌三维图像;A1~A3、N1~N3 分别为 3 时期 AOB和 NOB 三维图像。

FV1200显微镜激光束发射点位于样品下方, 故3D图像下层为生物膜最外层.由图3可以看出, 短程硝化不同时期生物膜上细菌空间分布大致相 同. 生物膜外层荧光强度最弱, 说明外层微生物分 布最少. 分析其原因, 外层生物膜直接与原水接 触,水质水量波动较大,生物膜易脱落,细菌不易 生长;同时,以胞外蛋白质指示胞外聚合物,做 CLSM 荧光染色分析, 如图 4(a) 所示, 图像下层为 生物膜最外层,该层蛋白质荧光强度最大, EPS 聚 集最多, 故生物膜外层细菌生长空间变少. 随着扫 描深度的增加,总菌、AOB、NOB 所代表的荧光强 度均有大幅度增加,说明微生物种群主要分布在生 物膜内部. 分析其原因, 生物膜内部环境更稳定, 菌群所需 DO 和基质都十分丰富, 适宜细菌增殖. 当激光束照射到直接与载体接触的最内层生物膜 时, 荧光稍有减少, 说明微生物菌落有所减少. 这 是因为生物膜上存在传质阻力, 使得传递到最内层 生物膜的 DO 和基质大大减少,细菌生长受到抑 制,故微生物数量和种类较少.

CLSM 分层扫面结果表明, MBBR 工艺生物膜厚度约 30 μm, 硝化细菌主要分布在生物膜表面的6~25 μm 处, AOB 和 NOB 分布位置并无明显区别. 另外, 观察图 3 中 A1~A3 和 N1~N3 发现AOB 和 NOB 硝化细菌层位于其他异养细菌层里面, 这是由于异养菌和硝化菌对生存基质的竞争导致生物膜结构出现分层现象^[14]. 比增殖速率更高的异养菌靠近生物膜外层,直接获取 DO 和有机碳源, 获得更多生存空间; 硝化细菌在较低 DO 下即可达到最大比生长速率, 故生长在异养菌内层. 另外, 外层异养菌作为内层硝化细菌的屏障, 也有一

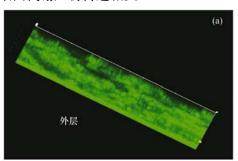


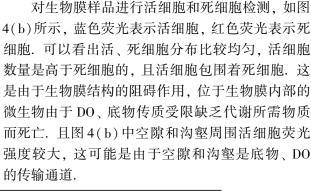
1. NAR = 10. 27%; 2. NAR = 52. 12%; 3. NAR = 94. 53%; T. 总菌; A. AOB; N. NOB

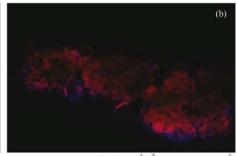
图 3 FISH 原位杂交 3D 照片

Fig. 3 FISH 3D images of simples

定保护作用. 更为重要的是, 异养细菌的内源呼吸作用会促使硝化层氧抑制的形成, 更易实现短程硝化. 异养菌增殖迅速、活性高, 分泌 EPS 多, 硝化细菌增殖慢、活性低, 分泌 EPS 少, 这也阐明了图4(a)中生物膜外层蛋白质含量最多的原因. 同时观察到生物膜内微生物分布是不均匀的, 而且许多细菌聚集在一起, 形成菌胶团. 且图 3 中生物膜上没有细菌分布的区域, 可能存在空隙和沟壑, 这些结构或与基质和细菌代谢产物传递相关.







(a) 蛋白质(FITC); (b)活细胞(Hoechst 33342), 死细胞(PI)

图 4 CLSM 荧光染色图

Fig. 4 CLSM fluorescent staining images

2.3 短程硝化实现过程中微生物菌落演替规律

图 3 显示了短程硝化不同时期,总菌、AOB 和 NOB 变化情况. 从中可以观察到, 总菌空间结构和 荧光强度变化不显著, AOB 和 NOB 变化较为明显. 第2 d NAR 为 10.27% 时, 生物膜中 AOB 和 NOB 均存在;随着短程硝化的实现,图 3 中 N1 和 N2 中 NOB 逐渐被洗脱, 但图 3 中 N3 仍含有少量 NOB, 说明比值控制(DO/NH4+N)可通过抑制 NOB 活性 可有效地实现短程硝化,并且短程硝化的实现在 NOB 未完全洗脱的基础上仍可以实现,这与 Bian 等[2]的结论是一致的, 但其也证实长期(>200 d) 采用比值控制策略, 反应器后期基本上检测不到 NOB. 与此同时, 观察到亚硝酸盐积累率提升的同 时, AOB 的数量逐渐增多. 比值控制高效地发挥氧 抑制作用, 使得 AOB 比增长速率高于 NOB, NOB 活性一直处于高抑制状态, AOB 受到较弱抑制, 经 过长期运行, 反应器中 AOB 得以富集.

通过对 NAR 为 10. 27%、52. 12% 和 93. 54% 时生物膜样品进行高通量测序,了解短程硝化实现过程中异养菌、AOB 和 NOB 等菌群变化. 侯爱月等^[15]和 Wagner等^[16]证实处理生活污水的微生物系统中变形菌门(Proteobacteria)和拟杆菌门(Bacteroidetes)为主要优势菌门,但拟杆菌门不含AOB 和 NOB,故不作讨论.高通量分析报告显示,

变形菌门中 β -变形菌门和 α -变形菌门的丰度最高, β -变形菌门包含 AOB、NOB、反硝化细菌和异养菌 $^{[17]}$,其中包含污水处理系统中最常见氨氧化菌 Nitrosomonas 和 Nitrosospira,因此可以认为富含 AOB 的生物膜样品 β -变形菌门丰度可能很高; α -变形菌门中 23% 为异养菌 $^{[18]}$,还包含常见 NOB 菌属 Nitrobacter. Nitrospira 为另一种典型 NOB 菌属,属硝化螺旋菌门 (phylum Nitrospira). Nitrosomonas 和 Nitrosospira 数量的总和计为 AOB,NOB以 Nitrobacter 和 Nitrospira 计,以"AOB/NOB"表征短程硝化性能. Shannon 指数和 Simpson 指数是用来估算微生物多样性的指数之一,Shannon 值越大,Simpson 值越小,微生物多样性越高.表 3 中列出短程硝化不同时期不同细菌占总菌比例及 AOB/NOB、Shannon、Simpson 变化情况.

观察表 3,在 NAR 逐步增长过程中, β -变形菌门在总菌中比例逐渐增大至 68. 17%,但 α -变形菌门所占比例由 23. 11% 锐减至 3. 99%,这与 β -变形菌门中 AOB 菌属的富集和 α -变形菌门中 NOB 的洗脱有一定的关系. 但 β -变形菌门和 α -变形菌门之和占总菌的比例均超过 70%,印证了变形菌门是污水处理系统的主要菌门. Nitrosomonas 菌属的含量逐步增加,但 Nitrosopira 的比例减少,可能是 Nitrosomonas 较高的比生长速率($0.088~h^{-1}$)和较好

表 3 短程硝化不同时期微生物种群特性

Table 3	Characteristics of	f microbial	population	during	different	periods of	partial	nitrification

NAR/%	eta-变形	α-变形	AOE	3/%	NOB	3/%	AOB ¹⁾ /NOB ²⁾	Shannon	Simspon
NAIL/ 70	菌门/%	菌门/%	Nitrosomonas	Nitrosospira	Nitrobacter	Nitrospira	AUD //NUD /	指数	指数
10. 27	52. 92	23. 11	2. 63	0.09	0. 04	1.36	1. 94	4. 98	0. 03
52. 17	57. 83	19.80	3. 17	0.06	0. 03	0.75	4. 14	4. 01	0.03
93. 54	68. 17	3.99	4. 98	0	0. 01	0.31	15. 56	3. 12	0.04

1) AOB 是 Nitrosomonas 和 Nitrosopira 在总菌中比例之和;2) NOB 是 Nitrobacter 和 Nitrospira 在总菌中比例之和

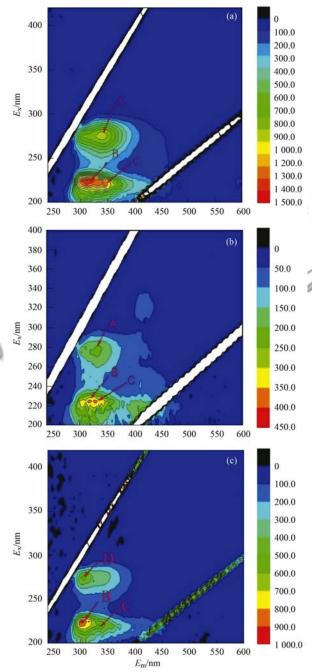
的环境适应性^[19], Nitrosospira 最大比生长速率仅为 0.033~0.035 h^{-1[20]}, 但 AOB 所占比例由 2.72% 增至 4.98%. NOB 菌属 Nitrobacter 和 Nitrospira 所占比例均在减少, AOB/NOB 比值递增至15.56, 说明生物膜反应器的硝化性能是逐步提升的. 同时发现, 短程硝化稳定运行的第 45 d, 生物膜中仍有 0.41%的 NOB 存在, 这与 FISH-CLSM 结果是一致的. Shannon 值下降了 1.86, Simpson 值增长了 0.01, 说明短程硝化实现过程中微生物多样性降低, 这可能是因为 AOB 的大量聚集, 消耗 DO 过多, 使得某些菌群生长受限; 也可能是NO₂-N积累, 对细胞起抑制作用的 FNA 浓度增大^[21,22], 部分菌群死亡.

2.4 生物膜 EEM 荧光光谱

由图 4 可以看出,生物膜表面 EPS 含量最多,既可富集环境营养物质传送至细胞,也可形成保护层以抵制不利因素的影响;生物膜内部 EPS 均匀分布,包裹着细胞,对支撑生物膜有着重要意义.有研究表明[23,241],短程硝化实现过程中,EPS产生量和化学结构会发生相应变化.图 5 是短程硝化实现过程中,不同时期(NAR 为 10.27%、52.12%、93.54%)生物膜 EPS 的 EEM 荧光光谱图. 荧光图谱波峰位置、荧光强度、化学成分及 PN、PS 变化情况总结在表 4 中.

结果显示,短程硝化实现期间,生物膜 EPS 都包含 3 种峰,即芳香性蛋白质 $I[E_x/E_m=(220\sim250)/(280\sim330)\,\mathrm{nm}]$ 、芳香性蛋白质 $II[E_x/E_m=(220\sim250)/(330\sim380)\,\mathrm{nm}]$ 和微生物沥出物 $[E_x/E_m=(250\sim280)/(290\sim380)\,\mathrm{nm}]$ 的特征峰,说明在运行过程中生物膜的 EPS 物质结构和组成变化不大. 但波峰位置、荧光强度和 PN、PS 值均有较大变化,说明亚硝酸盐的积累对 EPS 分泌会有一定影响. 其中峰 A、D 属于微生物沥出物,峰 B、C 属芳香性蛋白质. 短程硝化实现过程中,仅图 4(a)、5(b) 中特征峰 A 转化为图 5(c) 特征峰 D,化学成分由 Tryptophan PN-like 转化为 Tyrosine PN-like,戚

韩英等[25]证实 Tyrosine PN-like 的富集对生物脱氮



(a) NAR = 10. 27%; (b) NAR = 52. 12%; (c) NAR = 93. 54% 图 5 短程硝化不同时期 EPS 的 EEM 荧光光谱图

Fig. 5 EEM fluorescence spectra of EPS during different periods of partial nitrification

系统有至关重要的作用. 其中微生物沥出物指示细胞代谢产物, 微生物沥出峰荧光强度越高, 说明细胞代谢越旺盛. 观察表 4 发现, 运行过程中, A(C) 波峰荧光强度均先降低再增加, 这是由于起始生物膜反应器 DO 高达 7~8 mg·L⁻¹, 微生物活性较高, 分泌大量的 EPS, 故此时波峰荧光强度处于最高值, 且 PN 和 PS 值(以 VSS 计)分别高达 15.23 mg·g⁻¹和 24.16 mg·g⁻¹; 为实现短程硝化, 增强氧抑制, 反应器 DO 降至 2 mg·L⁻¹, 微生物活性降低, 分泌 EPS 量减少; 第 45 d 短程硝化已稳定运行 25 d, 适应低 DO 环境的 AOB 等菌大量增殖, EPS 分泌增多, 此时荧光强度和 PN、PS 值均有所回升.

而短程硝化过程中,生物膜上芳香性蛋白质的荧光强度均是最高的,其表示的是细胞物质的组成部分,表明在整个反应过程中,细胞更替是比较迅速的,尤其是 NAR 由 52. 12% 升至 93. 54% 期间,B 和 C 峰荧光强度各升高了 579. 63 和 145. 65,这与高通量分析报告中微生物种群多样性下降是相关的,可能是由于 NOB 和其他不耐高 FNA 菌群的衰亡.整个反应过程,并没有发现代表富里酸类物质 $[E_x/E_m=(220\sim250)/(380\sim480)\,\mathrm{nm}]$ 和腐殖酸类物质 $[E_x/E_m\geq250/(380\sim480)\,\mathrm{nm}]$,李延等 [5] 认为,腐殖酸类物质以溶解性为主,没有滞留在 EPS 中.

表 4 EPS 荧光元素及 PN、PS 变化

Table 4	Variation	of EPS	fluorescence	parameters,	PN	and	PS
---------	-----------	--------	--------------	-------------	----	-----	----

				-		
NAR/%	波峰	$E_{\rm x}/E_{\rm m}/{\rm nm}$	荧光强度	化学成分	PN(以VSS计)/mg·g ⁻¹	PS(以VSS計)/mg·g ⁻¹
	A	275/336	966.3	Tryptophan PN-like	15. 23	24.16
10.27	В	225/314	1 422.61	Aromatic PN-like	15. 23	24.16
	C	225/330	1 296.54	Aromatic PN-like	15.23	24. 16
	A	280/334	230.23	Tryptophan PN-like	8.00	9.98
52.12	В	225/324	404.6	Aromatic PN-like	8.00	9.98
	С	225/338	382.4	Aromatic PN-like	8.00	9.98
	D/	270/304	489.9	Tyrosine PN-like	12,71	11.72
93.54	B	225/304	962.03	Aromatic PN-like	12.71	11.72
61	(6)	220/336	635.55	Aromatic PN-like	12.71	11.72
				F. V 16	/ 4 1 / 4 1	

3 结论

- (1)采用 DO/NH_4^+ -N调控反应器工况,经过 20d 运行成功实现短程硝化,证实比值控制(DO/NH_4^+ -N)是实现短程硝化的有效手段.
- (2) 异养菌和硝化细菌共生于生物膜中, 既相 互竞争又相互影响, 外层为异养细菌, 内层为硝化 细菌.
- (3)在短程硝化的实现过程中,AOB 菌属主要是 Nitrosomonas,AOB/NOB 高达 15.56,成功实现AOB 富集、NOB 抑制.但稳定运行时期仍存在0.32%的 NOB,说明在 NOB 未完全洗脱的情况下,也可实现短程硝化.但反应器运行过程中微生物多样性下降,说明亚硝酸盐积累率升高的同时,可能抑制了某些种群活性.
- (4)反应器运行过程中, EPS 与微生物菌群变化息息相关. 微生物活性降低, EPS 分泌较少; 短程硝化稳定时期, NOB 等不耐 FNA 菌群衰亡, 芳香性蛋白质荧光强度下降. 但整个过程中, EPS 种类变化不明显.

参考文献:

- [1] 孙艺齐, 卞伟, 王盟, 等. 活性污泥法和生物膜法 SBR 工艺 亚硝化启动和稳定运行性能对比[J]. 环境科学, 2017, 38 (12): 5222-5228.
 - Sun Y Q, Bian W, Wang M, et al. Comparison of start-up and stable performance of nitritation in activated sludge process and biofilm process SBR process[J]. Environmental Science, 2017, 38(12): 5222-5228.
- [2] Bian W, Zhang SY, Zhang YZ, et al. Achieving nitritation in a continuous moving bed biofilm reactor at different temperatures through ratio control [J]. Bioresource Technology, 2017, 226: 73-79
- [3] Bartrolí A, Pérez J, Carrera J. Applying ratio control in a continuous granular reactor to achieve full nitritation under stable operating conditions [J]. Environmental Science & Technology, 2010, 44(23): 8930-8935.
- [4] Jemaat Z, Bartrolí A, Isanta E, et al. Closed-loop control of ammonium concentration in nitritation: convenient for reactor operation but also for modeling [J]. Bioresource Technology, 2013, 128: 655-663.
- [5] 李延,解迪,梁文艳,等. SBBR 反应器运行中生物膜胞外聚合物的变化特征[J]. 环境科学与技术,2016,39(4):95-101.
 - Li Y, Xie D, Liang W Y, et al. Variations of extracellular polymeric substances of bio-film in operation processes of SBBR [J]. Environmental Science & Technology, 2016, 39(4): 95-

- 101
- [6] 陈光辉. 生物脱氮包埋菌的制备及其在污水处理中的应用 [D]. 北京: 北京工业大学, 2016.
- [7] Wagner M, Ivleva N P, Haisch C, et al. Combined use of confocal laser scanning microscopy (CLSM) and Raman microscopy (RM): investigations on EPS-matrix [J]. Water Research, 2009, 43(1): 63-76.
- [8] 于莉芳, 杜倩倩, 傅学焘, 等. 城市污水中硝化菌群落结构与性能分析[J]. 环境科学, 2016, 37(11): 4366-4371.

 Yu L F, Du Q Q, Fu X T, et al. Community structure and activity analysis of the nitrifiers in raw sewage of wastewater treatment plants [J]. Environmental Science, 2016, 37(11): 4366-4371.
- [9] 王荣昌,文湘华,钱易. 悬浮载体生物膜内硝化菌群空间分布规律[J]. 环境科学,2006,27(11):2358-2362.
 Wang R C, Wen X H, Qian Y. Spatial distribution of nitrifying bacteria communities in suspended carrier biofilm [J]. Environmental Science, 2006, 27(11):2358-2362.
- [10] Schmid M, Thill A, Purkhold U, et al. Characterization of activated sludge flocs by confocal laser scanning microscopy and image analysis [J]. Water Research, 2003, 37(9): 2043-2052.
- [11] Greuter D, Loy A, Horne M, et al. Probebase-an online resource for rRNA-targeted oligonucleotide probes and primers; new features 2016 [J]. Nucleic Acids Research, 2016, 44 (D1); D586-D589.
- [12] Shi L, Günther S, Hübschmann T, et al. Limits of propidium iodide as a cell viability indicator for environmental bacteria[J]. Cytometry Part A, 2007, 71A(8): 592-598.
- [13] Zhang X J, Zhang H Z, Ye C M, et al. Effect of COD/N ratio on nitrogen removal and microbial communities of CANON process in membrane bioreactors [J]. Bioresource Technology, 2015, 189: 302-308.
- [14] Nogueira R, Melo L F, Purkhold U, et al. Nitrifying and heterotrophic population dynamics in biofilm reactors: effects of hydraulic retention time and the presence of organic carbon[J]. Water Research, 2002, 36(2): 469-481.
- [15] 侯爱月,李军,王昌稳,等. 不同好氧颗粒污泥中微生物群落结构特点[J]. 中国环境科学,2016,36(4):1136-1144.
 Hou A Y, Li J, Wang C W, et al. Characteristics of microbial
 - community structure in different aerobic granular sludge [J]. China Environmental Science, 2016, **36**(4): 1136-1144.
- [16] Wagner M, Loy A. Bacterial community composition and function in sewage treatment systems [J]. Current Opinion in Biotechnology, 2002, 13(3): 218-227.

- [17] Reino C, Suárez-Ojeda M E, Pérez J, et al. Kinetic and microbiological characterization of aerobic granules performing partial nitritation of a low-strength wastewater at 10°C [J]. Water Research, 2016, 101: 147-156.
- [18] Kindaichi T, Ito T, Okabe S. Ecophysiological interaction between nitrifying bacteria and heterotrophic bacteria in autotrophic nitrifying biofilms as determined by microautoradiography-fluorescence in situ hybridization [J]. Applied and Environmental Microbiology, 2004, 70(3): 1641-1650.
- [19] Terada A, Sugawara S, Yamamoto T, et al. Physiological characteristics of predominant ammonia-oxidizing bacteria enriched from bioreactors with different influent supply regimes [J]. Biochemical Engineering Journal, 2013, 79: 153-161.
- [20] Wei B, Li J, Hou A Y, et al. Rapidly startup of partial nitrification in sequencing batch reactor and microbiological analysis [J]. Desalination and Water Treatment, 2016, 57 (44): 21062-21070.
- [21] 韩晓宇, 张树军, 甘一萍, 等. 以 FA 与 FNA 为控制因子的 短程硝化启动与维持[J]. 环境科学, 2009, **30**(3); 809-814.
 - Han X Y, Zhang S J, Gan Y P, et al. Start up and maintain of nitritation by the inhibition of FA and FNA[J]. Environmental Science, 2009, 30(3): 809-814.
- [22] 委燕, 王淑莹, 马斌, 等. 缺氧 FNA 对氨氧化菌和亚硝酸盐 氧化菌的选择性抑菌效应[J]. 化工学报, 2014, **65**(10): 4145-4149. Wei Y, Wang S Y, Ma B, et al. Selective inhibition effect of free nitrous acid on ammonium oxidizing bacteria and nitrite oxidizing bacteria under anoxic condition [J]. CIESC Journal,
- [23] Wei D, Du B, Zhang J, et al. Composition of extracellular polymeric substances in a partial nitrification reactor treating high ammonia wastewater and nitrous oxide emission[J]. Bioresource Technology, 2015, 190: 474-479.

2014, 65(10): 4145-4149.

- [24] Zhang Z J, Chen S H, Wang S M, et al. Characterization of extracellular polymeric substances from biofilm in the process of starting-up a partial nitrification process under salt stress [J]. Applied Microbiology and Biotechnology, 2011, 89(5): 1563-1571.
- [25] 戚韩英. 影响好氧颗粒污泥形成与结构稳定的胞外多聚物关键组分研究[D]. 杭州: 浙江大学, 2012.
 - Qi H Y. Study of key component in extracellular polymeric substances during the formation and stability of aerobic granular sludge[D]. Hangzhou: Zhejiang University, 2012.

HUANJING KEXUE

Environmental Science (monthly)

Vol. 39 No. 3 Mar. 15, 2018

CONTENTS

Characterization and Variation of Organic Carbon (OC) and Elemental Carbon (EC) in PM _{2.5} During the Winter in the Yangtze Fi	tiver Delta Region, China ·····
Characterization and Variation of Organic Galloon (OC) and Electrical California (ED) in Fig. 5 During the Winter in the Fangue Fig.	
Important Effect of Secondary Inorganic Salt Extinction on Visibility Impairment in the Northern Suburb of Nanjing	
Day-Night Differences and Source Apportionment of Inorganic Components of PM _{2.5} During Summer-Winter in Changzhou City ·····	······ LIU Jia-shu, GU Yuan, MA Shuai-shuai, et al. (980)
Characteristics of Elements in PM _{2.5} and PM ₁₀ in Road Dust Fall During Spring in Tianjin	······ WANG Shi-bao, JI Ya-qin, LI Shu-li, et al. (990)
Particle Size Distribution and Human Health Risk Assessment of Heavy Metals in Atmospheric Particles from Beijing and Xinxiang	During Summer
	····· ZHANG Xin, ZHAO Xiao-man, MENG Xue-jie, et al. (997)
$ Ecological \ and \ Health \ Risks \ of \ Trace \ Heavy \ Metals \ in \ Atmospheric \ PM_{25} \ Collected \ in \ Wuxiang \ Town, \ Shanxi \ Province $	····· GUO Zhao-xia, GENG Hong, ZHANG Jin-hong, et al. (1004)
Characteristics of Particulate and Inorganic Elements of Motor Vehicles Based on a Tunnel Environment	
A 2013-based Atmospheric Ammonia Emission Inventory and Its Characteristic of Spatial Distribution in Henan Province	
Emission Characteristics of Wind Erosion Dust from Topsoil of Urban Roadside-Tree Pool	······ LI Bei-bei, QIN Jian-ping, QI Li-rong, et al. (1031)
Particulate Component Emission Characteristic from a Diesel Bus with DOC and CDPF	······ LOU Di-ming, GENG Xiao-yu, SONG Bo, et al. (1040)
Water Quality in the Henan Intake Area of the South-to-North Water Diversion Project	
Spatio-Temporal Patterns and Environmental Risk of Endocrine Disrupting Chemicals in the Liuxi River	······ FAN Jing-jing, WANG Sai, TANG Jin-peng, et al. (1053)
Fate and Origin of Major Ions in River Water in the Lhasa River Basin, Tibet	······ ZHANG Qing-hua, SUN Ping-an, HE Shi-yi, et al. (1065)
Identification of Nitrate Sources and the Fate of Nitrate in Downstream Areas: A Case Study in the Taizi River Basin	
Sources, Distribution of Main Controlling Factors, and Potential Ecological Risk Assessment for Heavy Metals in the Surface Sedim	ent of Hainan Island North Bay, South China
ZE	
Characteristics of Heavy Metals Pollution of Farmland and the Leaching Effect of Rainfall in Tianjin	
Seasonal Difference in Water Quality Between Lake and Inflow/Outflow Rivers of Lake Taihu, China	ZHA Hui-ming, ZHU Meng-yuan, ZHU Guang-wei, et al. (1102)
Characteristics of Nitrogen Release at the Sediment-Water Interface in the Typical Tributaries of the Three Gorges Reservoir During	the Sensitive Period in Spring
Spatial Distributions of Transferable Nitrogen Forms and Influencing Factors in Sediments from Inflow Rivers in Different Lake Basin	
Effects of Hydrological and Meteorological Conditions on Diatom Proliferation in Reservoirs	
Vertical Distribution of Fungal Community Composition and Water Quality During the Deep Reservoir Thermal Stratification S	
Community Structure and Influencing Factors of Bacterioplankton in Spring in Zhushan Bay, Lake Taihu	XUE Yin-gang, LIU Fei, SUN Meng, et al. (1151)
Characteristics of Sediment Oxygen Demand in a Drinking Water Reservoir	SU Lu, HUANG Ting-lin, LI Nan, et al. (1159)
Effects of Wastewater Nitrogen Concentrations and NH ₄ ⁺ /NO ₃ ⁻ on Nitrogen Removal Ability and the Nitrogen Component of Myriop	hyllum aquaticum (Vell.) Verde ·····
4 3 0 7 0 1 7 1	··· MA Yong-fei, YANG Xiao-zhen, ZHAO Xiao-hu, et al. (1167)
Effect of Nutrient Loadings on the Regulation of Water Nitrogen and Phosphorus by Vallisneria natans and Its Photosynthetic Fluores	scence Characteristics ·····
Enter of Francisco and To Topical of Water Francisco and Transporter by Francisco and To Topical of Transporter by Francisco and To Topical of Topical of Transporter by Francisco and Topical of Topi	···· ZHOU Yi-wen, XU Xiao-guang, HAN Rui-ming, et al. (1180)
Removal of Organic Matter from Water by Chemical Preoxidation Coupled with Biogenic Manganese Oxidation	··· JIAN Zhi-yu, CHANG Yang-yang, WANG Li-xin, et al. (1188)
Treating Simulated Dye Wastewater by an In Situ Copper Ferrite Process	······· HAN Zhi-yong, HAN Kun, HAO Hao-tian, et al. (1195)
Experiment to Enhance Catalytic Activity of α-FeOOH in Heterogeneous UV-Fenton System by Addition of Oxalate	·· MIAO Xiao-zeng, DAI Hui-wang, CHEN Jian-xin, et al. (1202)
Fabrication of a Biomass-Based Hydrous Zirconium Oxide Nanocomposite for Advanced Phosphate Removal	QIU Hui, QIN Zhi-feng, LIU Feng-ling, et al. (1212)
Characteristic of Nitrate Adsorption in Aqueous Solution by Iron and Manganese Oxide/Biochar Composites	· ZHENG Xiao-qing, WEI An-lei, ZHANG Yi-xuan, et al. (1220)
Preparation of PAAm/HACC Semi-Interpenetrate Network Hydrogel and Its Adsorption Properties for Humic Acid from Aqueous Sol	
Groundwater Arsenic and Silicate Adsorption on TiO ₂ and the Regeneration of TiO ₂	MA Wen-jing, YAN Li, ZHANG Jian-feng (1241)
Removal Efficiency and Mechanism of Removal by Humic Acid of the Integrated Floc-ultrafiltration Process	
Emission Inventory of Greenhouse Gas from Urban Wastewater Treatment Plants and Its Temporal and Spatial Distribution in China	··········· YAN Xu, QIU De-zhi, GUO Dong-li, et al. (1256)
Start-up and Operation of Biofilter Coupled Nitrification and CANON for the Removal of Iron, Manganese and Ammonia Nitrogen ·	LI Dong, CAO Rui-hua, YANG Hang, et al. (1264)
Analysis of CANON Process Start-up with Fiber Carrier	GU Cheng-wei, CHEN Fang-min, LI Xiang, et al. (1272)
Characteristics of Biofilm During the Transition Process of Complete Nitrification and Partial Nitrification	
Effect of Intermediate-Setting Aeration on the CANON Granular Sludge Process in the AUSB Reactor	CHENG Shuo, LI Dong, ZHANG Jie, et al. (1286)
Effect of Organic Carbon Source on Start-up and Operation of the CANON Granular Sludge Process	LI Dong, WANG Yan-ju, LÜ Yu-feng, et al. (1294)
Start-Up and Regional Characteristics of a Pilot-scale Integrated PN-ANAMMOX Reactor	
Effect of NO, -N Recycling Ratio on Denitrifying Phosphorus Removal Efficiency in the ABR-MBR Combined Process	
Effects of Magnetic Fe ₃ O ₄ Nanoparticles on the Characteristics of Anaerobic Granular Sludge and Its Interior Microbial Community	
Characterization Composition of Soluble Microbial Products in an Aerobic Granular Sludge System	
Influence of Ciprofloxacin on the Microbial Community and Antibiotics Resistance Genes in a Membrane Bioreactor	
Analysis of Low C/N Wastewater Treatment and Structure by the CEM-UF Combined Membrane-Nitrification/Denitrification System	
	· XING lin-liang, ZHANG Yan, CHEN Chang-ming, et al. (1342)
Effects of Phosphorus on the Activity and Bacterial Community in Mixotrophic Denitrification Sludge	
Acclimatization and Community Structure Analysis of the Microbial Consortium in Nitrate-Dependent Anaerobic Methane Oxidation	1, , , , ,
Diffusion of Microorganism and Main Pathogenic Bacteria During Municipal Treated Wastewater Discharged into Sea	
Oxytetracycline Wastewater Treatment in Microbial Fuel Cells and the Analysis of Microbial Communities	
Spatial and Temporal Variability of Soil C-to-N Ratio of Yugan County and Its Influencing Factors in the Past 30 Years	
Spatial Heterogeneity of Soil Carbon and its Fractions in the Wolfberry Field of Zhongning County	
Response of Soil Enzyme Activities and Their Relationships with Physicochemical Properties to Different Aged Coastal Reclamation	
recoponed or con analytic recurred and then rectanonemps with rhysicoenical rioperies to different riger Coastal rectalliation	VIE Vuo fong DILLi iio WANC Oi gi et al. (1404)
Distribution, Sources, and Ecological Risk Assessment of Polycyclic Aromatic Hydrocarbons (PAHs) in Soils of the Central and E	astern Areas of the Oinghai-Tibetan Plateau ·····
Distribution, Sources, and Ecological Risk Assessment of Polycyclic Aromatic Hydrocarbons (PAHs) in Soils of the Central and E	astern Areas of the Qinghai-Tibetan Plateau
Distribution, Sources, and Ecological Risk Assessment of Polycyclic Aromatic Hydrocarbons (PAHs) in Soils of the Central and E Source Apportionment of Heavy Metals in Farmland Soils Around Mining Area Based on UNMIX Model	astern Areas of the Qinghai-Tibetan Plateau
Distribution, Sources, and Ecological Risk Assessment of Polycyclic Aromatic Hydrocarbons (PAHs) in Soils of the Central and E	astern Areas of the Qinghai-Tibetan Plateau